

Metastasis in context

Citation for published version (APA):

Sleeboom, J. J. F., Amirabadi, H. E., Nair, P., Sahlgren, C. M., & Den Toonder, J. M. J. (2018). Metastasis in context: modeling the tumor microenvironment with cancer-on-a-chip approaches. *Disease Models & Mechanisms*, 11(3), Article 033100. <https://doi.org/10.1242/dmm.033100>

DOI:

[10.1242/dmm.033100](https://doi.org/10.1242/dmm.033100)

Document status and date:

Published: 01/03/2018

Document Version:

Accepted manuscript including changes made at the peer-review stage

Please check the document version of this publication:

- A submitted manuscript is the version of the article upon submission and before peer-review. There can be important differences between the submitted version and the official published version of record. People interested in the research are advised to contact the author for the final version of the publication, or visit the DOI to the publisher's website.
- The final author version and the galley proof are versions of the publication after peer review.
- The final published version features the final layout of the paper including the volume, issue and page numbers.

[Link to publication](#)

General rights

Copyright and moral rights for the publications made accessible in the public portal are retained by the authors and/or other copyright owners and it is a condition of accessing publications that users recognise and abide by the legal requirements associated with these rights.

- Users may download and print one copy of any publication from the public portal for the purpose of private study or research.
- You may not further distribute the material or use it for any profit-making activity or commercial gain
- You may freely distribute the URL identifying the publication in the public portal.

If the publication is distributed under the terms of Article 25fa of the Dutch Copyright Act, indicated by the "Taverne" license above, please follow below link for the End User Agreement:

www.tue.nl/taverne

Take down policy

If you believe that this document breaches copyright please contact us at:

openaccess@tue.nl

providing details and we will investigate your claim.

Metastasis in context: Modeling the tumor microenvironment with cancer-on-a-chip approaches

Jelle J.F. Sleeboom^{123†}, Hossein Eslami Amirabadi^{13†}, Poornima Nair¹³,
Cecilia M. Sahlgren²³⁴, Jaap M.J. den Toonder^{13*}

ABSTRACT

Most cancer deaths are not caused by the primary tumor, but by secondary tumors formed through metastasis, a complex and poorly understood process. Cues from the tumor microenvironment, such as the biochemical composition, cellular population, extracellular matrix, and tissue (fluid-) mechanics, have been indicated to play a pivotal role in the onset of metastasis. Dissecting the role of these cues from the tumor microenvironment in a controlled manner is challenging, but essential to understanding metastasis. Recently, cancer-on-a-chip models have emerged as a tool to study the tumor microenvironment and its role in metastasis. These models are based on microfluidic chips and contain small chambers for cell culture, enabling control over local gradients, fluid flow, tissue mechanics, and composition of the local environment. Here, we review the recent contributions of cancer-on-a-chip models to our understanding of the role of the tumor microenvironment in the onset of metastasis, and provide an outlook for future applications of this emerging technology.

KEY WORDS: Cancer-on-a-chip, microfluidics, tumor microenvironment, cancer, metastasis

SUMMARY STATEMENT: This review evaluates the recent contributions of cancer-on-a-chip models to our understanding of the role of the tumor microenvironment in the onset of metastasis, and provides an outlook for future applications of this emerging technology.

¹Microsystems group, Department of Mechanical Engineering, Eindhoven University of Technology, Gemini-Zuid, Groene Loper 15, 5612AZ, Eindhoven, the Netherlands

²Soft Tissue Engineering & Mechanobiology, Eindhoven University of Technology, Gemini-Zuid, Groene Loper 15, 5612AZ, Eindhoven, the Netherlands

³Institute for Complex Molecular Systems, Eindhoven University of Technology, Gemini-Zuid, Groene Loper 15, 5612AZ, Eindhoven, the Netherlands

⁴Åbo Akademi University, Domkyrkotorget 3, FI-20500, Turku, Finland

† These authors contributed equally to this work.

* Corresponding author, email: J.M.J.d.Toonder@tue.nl

33 Introduction

34 For decades, researchers studying cancer have been focusing mainly on the genetic origin of the disease, which
35 has led to major advances in cancer detection and treatment. Despite the increasingly effective therapeutic
36 approaches, cancer is still one of the deadliest diseases in the world, accounting for nearly 1 in 6 of all deaths
37 worldwide (WHO Cancer fact sheet, who.int/mediacentre/factsheets). A main challenge in treating cancer is that most
38 deaths are not caused by the primary tumor, but by secondary tumors that are formed through metastasis. In this
39 step-wise process, cancer cells go through invasion, intravasation and extravasation (Box 1, Glossary), to
40 ultimately form a secondary tumor, as detailed in Figure 1A. Yet we only partially understand the full complexity
41 of the metastasis process, reviewed in (Joyce and Pollard, 2009).

42 We do know that metastasis is not only driven by intrinsic factors such as the (epi-)genetic characteristics of
43 the cancer cells, but is also critically affected by cell-extrinsic factors mediated by the tumor microenvironment
44 (TME; Box 1) reviewed in (Hanahan and Weinberg, 2011). In this review, we focus on the role of the TME in
45 driving tumor invasion, angiogenesis (Box 1) and intravasation into the vasculature, thereby initiating cancer cell
46 dissemination throughout the body. A major challenge in understanding the role of the TME is that a systematic
47 analysis of the influence of individual TME components is still very difficult to achieve.

48 Current experimental approaches to study cancer invasion are *in vitro* 2D or 3D cell cultures, complemented
49 with *in vivo* animal models using human cell lines or patient-derived xenografts, reviewed in (Alemany-Ribes and
50 Semino, 2014; Choi et al., 2014). These approaches have been important for our current understanding of cancer,
51 but they also have some limitations. Most importantly, growing cells in 2D culture models does not capture the
52 3D nature of tumors, and leads to deviating cellular behavior, reviewed in (Weigelt et al., 2014). Current 3D
53 models, such as cancer spheroids and 3D hydrogel cultures, have greatly improved upon this, and are often
54 compatible with the methodologies for 2D models, enabling the use of conventional experimental read-outs.
55 However, a disadvantage of current 3D models is the static (non-flow) nature of these models, which limits the
56 researchers' control over local biochemical gradients, but is also very different from the vascularized *in vivo*
57 tissue. Additionally, most 3D models are mono-cellular and do not include other cell types typically found in the
58 TME. Animal models intrinsically contain a more complete representation of the *in vivo* TME complexity, yet
59 their use is less straightforward: they are generally inefficient, expensive, and not always a good representation of
60 human (patho-)physiology.

61 To complement the current research models and overcome some of their limitations, several groups are
62 developing and using so-called cancer-on-a-chip models (CoC, Box 2). In this review, we discuss the current
63 status of CoC research, particularly in relation to our current knowledge about the role of the TME in the onset of
64 metastasis. We briefly revisit the TME as we understand it from traditional *in vitro* and *in vivo* research models,
65 after which we review the contributions of CoC models in more detail. Furthermore, we highlight the most

66 important outstanding challenges regarding the interactions between cancer cells and their environment, and
67 discuss how future developments in CoC technology could contribute to tackling these challenges.

68 The tumor microenvironment

69 Here, we categorize the factors that define the TME into four groups (Figure 1B-E): (1) biochemical cues, or the
70 soluble factors affecting cancer cells; (2) other cell types in the TME, such as immune cells and fibroblasts; (3)
71 the extracellular matrix (ECM; Box 1); (4) mechanical cues, such as interstitial fluid flow. We briefly review what
72 is known and unknown about the significance of these factors for cancer invasion, angiogenesis, and
73 intravasation, on the basis of current research models, such as conventional *in vitro* cell cultures and animal
74 models.

75 Intrinsic biochemical changes in the TME

76 In solid tumors, solute transport is limited, but energy demands and waste generation are high. This discrepancy
77 results in gradients arising throughout the tumor (Figure 1B). Here, we highlight the solutes that are known to
78 affect cancer cells: oxygen and metabolic products.

79 Oxygen gradients and hypoxia

80 When exposed to hypoxic (low oxygen) conditions in the tumor, cells activate several mechanisms to avert
81 hypoxia-induced apoptosis. One such example is angiogenesis induced via hypoxia inducible growth factor (HIF)
82 1-alpha. This transcription factor affects the expression of genes responsible for angiogenesis, cell survival, cell
83 metabolism, and invasion, reviewed in (Semenza, 2003). In the context of invasion, the most direct downstream
84 effects of HIF 1-alpha overexpression are the epithelial–mesenchymal transition (EMT; Box 1), and increased
85 amoeboid invasion (Box 1) in epithelial cancers (Lehmann et al., 2017). Additionally, hypoxia can affect cancer
86 cell invasion by activating other stromal cells and by remodeling the ECM, reviewed in (Semenza, 2016).

87 Cancer cell metabolism and extracellular acidity

88 A distinct difference between cancer and healthy cells is found in their metabolism: due to the above-mentioned
89 limited transport of solutes within a tumor, cancer cells rely on less efficient pathways to generate energy. This
90 difference, referred to as the Warburg effect (Box 1), causes an elevation in both the extracellular acidity and
91 lactate concentration. There is growing evidence that this increases the invasiveness of cancer cells, reviewed in
92 (Kato et al., 2013). Moreover, elevated extracellular acidity has been shown to negatively affect the healthy tissue
93 surrounding breast, prostate, and colon tumor xenografts, making it more susceptible to cancer cell invasion
94 (Estrella et al., 2013; Gatenby et al., 2006; Rofstad et al., 2006). Lactate was found to have similar effects on
95 carcinoma cells *in vitro* (Goetze et al., 2011).

96 Oxygen, extracellular acidity, and lactate clearly have links to metastasis, but studying the impact of these
97 biochemical gradients is still challenging using conventional approaches.

98 Cellular components of the tumor microenvironment

99 This section highlights the most studied cells in the TME: inflammatory cells, cancer associated fibroblasts (CAF;
100 Box 1), and endothelial cells (Figure 1C).

101 Inflammatory cells

102 Cancer cells and TME stromal cells recruit inflammatory cells from the circulation, reviewed in (Balkwill and
103 Mantovani, 2001; Coussens and Werb, 2002; Mantovani et al., 2008). These cells can have both tumor-
104 suppressing and -promoting effects (Coussens and Werb, 2002; Mantovani et al., 2008). Among the immune cells
105 in the TME, macrophages are the most abundant, as reviewed in (Hu et al., 2016), and we discuss them in more
106 detail here.

107 Tumor associated macrophages (TAMs; Box 1), which derive from recruited circulating monocytes, reviewed
108 in (Hu et al., 2016; Mantovani and Sica, 2010), can have two phenotypes: M1 and M2. Depending on this
109 phenotype, which is highly influenced by cues from the TME, TAMs can have contrasting roles in cancer,
110 reviewed in (Lewis and Pollard, 2006; Mosser and Edwards, 2008; Sica et al., 2008). M1 macrophages generally
111 have pro-inflammatory tumor-suppressing properties in the early stages of cancer, but they polarize towards the
112 M2 phenotype as the tumor progresses. These M2 TAMs secrete cytokines and growth factors to suppress anti-
113 tumor inflammatory activities, reviewed in (Mantovani et al., 2002; Sica et al., 2008). In addition, they can
114 directly promote invasion, secrete pro-angiogenic factors, such as vascular endothelial growth factor (VEGF) (Lin
115 et al., 2006), and remodel the ECM by expressing and activating matrix metalloproteinases (MMPs; Box 1)
116 (Sangaletti et al., 2003).

117 Pro-tumor activity of the TAMs makes them a proper target for anti-tumor therapies, reviewed in (Belgiovine
118 et al., 2016; Mantovani and Allavena, 2015). For example, M2 TAMs can be switched to the M1 type to trigger
119 anti-tumor response of the immune system (Buhtoiarov et al., 2011; Rolny et al., 2011). However, therapeutic
120 treatments can also trigger TAMs towards a more tumor-supporting function (Dijkgraaf et al., 2013), so better
121 models are needed to increase our insight in the effects of drugs on TAMs. In addition, work in conventional
122 model systems revealed much about the role of TAMs, but it is important to recognize that most of our current
123 knowledge is based on mouse models. Species-specific differences might affect TAM recruitment and activation
124 mechanisms, reviewed in (Ostuni et al., 2015), thereby hampering the translation of this knowledge into the
125 context of human cancer.

126 Cancer associated fibroblasts

127 Cancer associated fibroblasts (CAFs) are extremely abundant in the tumor stroma. They are recruited and
128 activated by cancer cells, reviewed in (Xouri and Christian, 2010). In healthy tissues, fibroblasts are responsible
129 for ECM deposition, regulating epithelial differentiation, inflammation, and wound healing, reviewed in (Cirri
130 and Chiarugi, 2012; Darby and Hewitson, 2007; Parsonage et al., 2005). In tumors, CAFs have been shown to

131 enhance cancer cell proliferation, invasion, and angiogenesis, reviewed in (Kalluri and Zeisberg, 2006; Kuzet and
132 Gaggioli, 2016; Räsänen and Vaheri, 2010; Shimoda et al., 2010). Together with cancer cells, CAFs re-organize
133 the ECM, potentially contributing to most of the exogenous EMT stimuli during cancer invasion, reviewed in
134 (Bhowmick et al., 2004; Cirri and Chiarugi, 2012). As they are directed by pro-fibrotic signals from the cancer
135 cells, they partly govern the volume and composition of the tumor stroma (Kalluri and Zeisberg, 2006). CAFs
136 appear to be very similar to activated fibroblasts in wound healing, but it is unclear if this means that they are the
137 same cell type, or if CAFs acquire properties that are unique to the TME, reviewed in (Bierie and Moses, 2006;
138 Darby and Hewitson, 2007). Furthermore, the role of mechanotransduction in CAF activation is not yet fully
139 understood (Kuzet and Gaggioli, 2016).

140 Since CAFs are genetically more stable than cancer cells and they play an important role in cancer metastasis,
141 they are an interesting target for cancer therapy (Cirri and Chiarugi, 2012). For example, the bilateral signalling
142 between cancer cells and CAFs can be inhibited to prevent cancer invasion, reviewed in (Tao et al., 2017).

143 Endothelial cells

144 In solid tumors, angiogenesis is a process that accompanies and supports tumor growth, and is characterized by
145 the development of heterogeneous, chaotic, distorted, and leaky vessel networks (Hanahan and Weinberg, 2011;
146 Nagy et al., 2010). The new vessels provide the tumor with oxygen, nutrients and waste disposal, and facilitate
147 cancer cell intravasation. As such, targeting angiogenesis to oppose cancer progression has received considerable
148 attention, and trials with angiogenesis inhibiting drugs are in progress. Angiogenesis can be induced via
149 angiogenic factors, such as VEGF-A and angiopoietin-2 (ANGPT2), reviewed in (Semenza, 2013). Similarly, the
150 formation of lymphatic vessels can be induced by VEGF-C and VEGF-D, reviewed in (Van Zijl et al., 2011).
151 Recently, endothelial cells (ECs) have been proposed to directly affect cancer progression through angiocrine
152 signaling, reviewed in (Butler et al., 2010), and paracrine signaling (Cao et al., 2014). The idea of angiocrine
153 signaling is supported by *in vitro* data showing that ECs enhance the metastatic potential of cancer cells (Ghiabi et
154 al., 2014), but the *in vivo* relevance of this finding is not yet clear. Additionally, the mechanisms that underlie
155 endothelial barrier transmigration in the complex TME are not yet fully understood. It is important to recognize
156 that endothelial and other TME cells do not act in isolation, but are continuously in contact with their
157 surroundings. For example, ECs can dramatically affect the biochemical gradients in the TME, or the supply of
158 inflammatory cells, by altering blood flow.

159 **The extracellular matrix in cancer**

160 The ECM is the non-cellular component in all tissues and organs that provides cells with chemical and
161 mechanical support (Figure 1D), reviewed in (Bissell et al., 1982; Frantz et al., 2010). Dynamic cross-talk
162 between the cells and the ECM maintains tissue homeostasis (Bissell et al., 1982). In tumors however,
163 microenvironmental stimuli, such as hypoxia and solid stresses (Box 1), drive excessive matrix remodeling, as

164 illustrated in Figure 1D, reviewed in (Lu et al., 2012). This remodeling is a result of basement membrane (BM;
165 Box 1) and interstitial ECM degradation by overexpressed matrix-degrading enzymes, such as MMPs, reviewed
166 in (Deryugina and Quigley, 2006; Vihinen and Kähäri, 2002), by the increased deposition of new matrix
167 components, and by lysyl oxidase (LOX)-dependent crosslinking of ECM proteins (Cox et al., 2013).

168 Remodeling leads to changes in the physical properties of the ECM, such as increased stiffness, which plays an
169 important role in cancer progression, reviewed in (Butcher et al., 2009; Kumar and Weaver, 2009; Paszek and
170 Weaver, 2004). Increased matrix stiffness has been linked to increased cell traction forces that fuel cell migration,
171 reviewed in (Paszek et al., 2005), to malignant transformation, and to activation of the EMT program (Leight et
172 al., 2012; Paszek et al., 2005). Additionally, tumor growth leads to thinning and softening of the BM, which could
173 help cancer cells to invade through this barrier (Butcher et al., 2009; Kumar and Weaver, 2009; Paszek and
174 Weaver, 2004).

175 Like ECM stiffness, ECM topography is highly dynamic. Aligned ECM fibers and weakened microtracks are a
176 typical sign of invasive tumors (Friedl and Wolf, 2008). Furthermore, a remodeled matrix topography affects the
177 stability and bioavailability of ligands on the ECM fibers, as well as the accessibility of growth factors and
178 cytokines, thereby influencing tumor development, reviewed in (Egeblad et al., 2010; Hynes, 2009).

179 Due to the complexity of the cancer cell-ECM interactions, understanding the reciprocal relationship between
180 the matrix and cancer cells is still challenging: ECM remodeling can promote invasion, but is itself also induced
181 by invasion, reviewed in (Kumar and Weaver, 2009). New therapies targeting the ECM require a better
182 understanding of the cell-ECM interaction. For example, a deeper insight on this interaction can result in more
183 effective therapies that inhibit the degradation and production of the ECM during cancer invasion (Chen et al.,
184 2017; Cox et al., 2013). Within the TME, the ECM also indirectly relays mechanical cues to cancer cells, such
185 that changes in stiffness and topography can change how mechanical cues affect the tumor.

186 **Mechanical cues in the tumor microenvironment**

187 Mechanical cues, such as fluid pressure, shear stress, solid stresses, reviewed in (Koumoutsakos et al., 2013;
188 Kumar and Weaver, 2009), and tissue level deformations, especially relevant in tissues subject to dynamical
189 loading, such as the colon (Whitehead et al., 2008), can affect cancer cells.

190 In most solid tumors, the interstitial fluid pressure (IFP) is elevated due to the leaky vasculature and the
191 increased stiffness of the ECM, reviewed in (Shieh and Swartz, 2011). Generally, an elevated IFP leads to an
192 increase in the interstitial flow velocity, especially at the tumor-stroma interface, which has been linked to
193 increased cancer cell invasion in patients (Hompland et al., 2014).

194 Other mechanical cues originate from deformation at the tissue level. An example of this is the cyclic tensile
195 strain in the lung, which occurs during breathing and has been shown to affect the drug responsiveness of lung
196 cancer cells (Hendricks et al., 2012). Although direct therapeutic intervention in mechanical cues is not

197 straightforward, indirect methods to affect tissue stresses and IFP, for example via LOX inhibition (Cox et al.,
198 2013), could be employed for metastasis prevention. However, the full impact of tissue-level mechanical cues on
199 cancer cell invasion has not been studied in detail, since introducing these in an *in vitro* model is challenging.

200 The contribution of Cancer-on-a-chip

201 Although conventional models have provided a major contribution to our knowledge on metastasis, CoC models
202 have started to yield new insights into the role of the TME in metastasis initiation in recent years. Here, we review
203 the contributions of CoC models for each of the TME components that we defined above. We have categorized
204 the different CoC designs in 5 groups, as detailed in Figure 2. Figure 3 illustrates how these designs are operated
205 in practice, showing a number of concrete examples from the literature. Researchers generally choose between the
206 2D, lumen, compartmentalized, Y, or membrane chips based on which TME cues they are studying. However, the
207 basic components for a CoC remain the same: a microfluidic chip (Box 1), cancer cells, other cell types
208 (optional), matrix materials (optional), and equipment to control fluid flow, such as a syringe pump (optional).
209 The controlled parameters and read-out methods can differ between chip types, but common read-outs are based
210 on cell and invasive lesion tracking, gradient sensing, staining, and gene expression quantification using real-time
211 polymerase chain reaction (RT-PCR; Figure 3). For an overview of the available literature in table format, we
212 refer the reader to the Supplementary table.

213 Modeling intrinsic biochemical changes in the tumor

214 Oxygen gradients and hypoxia

215 Different methods have been used to generate oxygen gradients based on the steady-state diffusion of oxygen
216 from high to low concentration. A locally created balance between a source and a sink of oxygen can control both
217 gradient magnitude and direction.

218 This can be achieved in 2D chips using chemicals, either inside the cell culture channel (Wang et al., 2013), or
219 in parallel channels (Chen et al., 2011; Wang et al., 2015a). Examples of a parallel microchannel design and live
220 oxygen detection are shown in Figure 3F and M, respectively (Chen et al., 2011). Typical examples of scavenging
221 chemicals are pyrogallol combined with NaOH, and sodium sulphite, whereas typical oxygen sources are the
222 environment, or H₂O₂ combined with NaClO. A CoC approach using parallel channels could successfully
223 determine the effectiveness of several therapeutic agents as a function of the oxygen tension, which could be
224 useful in drug response studies. In this type of device, however, gradients remain stable as long as the chemicals
225 are continuously refreshed to maintain the reaction, which has the downside that reaction waste is continuously
226 produced.

227 Alternatively, waste-free gas supply channels can be used as sources and sinks of oxygen. Based on this
228 method, a gradient across a 3D hydrogel (Oppegard and Eddington, 2013) and a gradient across a

229 compartmentalized chip with a collagen ECM and a vessel-mimicking channel (Acosta et al., 2014) could be
230 generated. Using the compartmentalized chip, Acosta et al. determined cancer cell invasiveness as a function of
231 oxygen concentration. Other researchers enhanced local gradient control, by limiting environmental oxygen influx
232 using impermeable layers in the device (Chang et al., 2014; Funamoto et al., 2012), and thus enabled more
233 accurate quantification of the oxygen response. Interestingly, using a 2D chip, researchers found evidence of a
234 direct influence of oxygen gradients on the direction of cell migration in A549 lung carcinoma cells, who tended
235 to migrate towards lower oxygen concentration, termed aerotaxis (Chang et al., 2014). Similarly, MDA-MB-231
236 breast cancer cells were recently found to respond to aerotaxis, but in the opposite direction, towards higher
237 oxygen concentration. However, the 2D chip design in this study lacked oxygen control, which limited its ability
238 to draw conclusions on the relevance of aerotaxis in this cancer cell type (Yahara et al., 2016). If aerotaxis is
239 persistent across cancer cell types, but with different directionality, it could have a direct impact on the
240 effectiveness of therapies such as angiogenesis inhibition for different cancers.

241 Cancer cell metabolism and extracellular acidity

242 Currently, little work has focused on investigating the metabolism-related concentration gradients in CoC
243 systems. To our knowledge, active control over acidity or acid/lactate gradients has not been shown. However,
244 some work has been done on quantifying the concentration and distribution of metabolites inside 2D and Y chips
245 (Walsh et al., 2009; Xu et al., 2015), highlighting that microfluidics hold the potential to advance this field.

246 **Modeling the cellular environment of the tumor**

247 Tumor associated macrophages

248 Macrophage-mediated cancer cell invasion has been one of the most frequently studied applications of CoC
249 models. Zervantonakis et al. cultured cancer cells, macrophages and endothelial cells in a compartmentalized
250 chip, shown in Figure 3H (Zervantonakis et al., 2012). They observed that TAMs significantly increased the
251 ability of cancer cells to impair the endothelial cell barrier and intravasate. Bai et al. used a similar design to
252 investigate TAM-mediated activation of EMT, and found that different TAM subtypes can disperse cancer cell
253 aggregates via different mechanisms (Bai et al., 2015). For example, they observed that a subtype of M2
254 macrophages could only promote aggregate dispersion through direct contact.

255 Several CoC-based publications also show that cancer cells directly affect TAMs, increasing the migration and
256 affecting the polarization of resident macrophages (Huang et al., 2009; Zhao et al., 2015). For instance, Huang et
257 al. used a compartmentalized chip and observed that invasive cancer cells recruited macrophages rather than
258 migrating towards them.

259 These studies show that CoC devices can help us understand the activation of the TAMs, and how these
260 macrophages enhance cancer invasion.

261 Cancer associated fibroblasts

262 Real-time imaging in CoC models has been used to study how CAFs affect cancer cell migration (Liu et al., 2007;
263 Ma et al., 2010; Truong et al., 2016; Yu et al., 2016). Typically, cell tracking techniques are used to analyze
264 cancer cell migration, as illustrated in Figure 3K (Truong et al., 2016). For example, Liu et al. observed collective
265 cell migration of adenoid cystic carcinoma cells into BM matrices when co-cultured with CAFs in a
266 compartmentalized chip. This behavior was repressed when MMP expression was inhibited in both cell types,
267 implying that MMP-mediated matrix proteolysis is critical to cancer invasion (Liu et al., 2007). In a different
268 study, in which CAFs and cancer cells were co-cultured in a compartmentalized chip, CAFs were shown to lead
269 the forefront of cancer cell migration into a BM matrix (Li et al., 2016). In another study, Sung et al. used a Y
270 chip to culture non-invasive mammary ductal carcinoma cells in the proximity of fibroblasts, shown in Figure 3I
271 (Sung et al., 2011). They controlled the distance between the cancer cells and fibroblasts and observed that the
272 cancer cells' transition to an invasive phenotype depends on this distance. The same group used a hybrid lumen-
273 compartment chip and observed the transition of non-invasive ductal carcinoma cells to an invasive phenotype
274 only when these cells are cultured with fibroblasts (Bischel et al., 2015). In contrast, negligible cancer cell
275 invasion was observed in a membrane chip that contained carcinoma spheroids and mammary epithelial cells in
276 one compartment, with fibroblasts in an adjacent compartment, as shown in Figure 3J (Choi et al., 2015). In
277 addition, several publications showed trans-differentiation of fibroblasts to activated fibroblasts when they were
278 co-cultured with cancer cells (Gioiella et al., 2016; Hsu et al., 2011; Ma et al., 2010).

279 So far, these CoC models have helped us to better understand the invasion-related interactions between CAFs
280 and cancer cells, highlighting the importance of CAFs in promoting cancer cell metastasis.

281 Endothelial cells

282 Several CoC-based studies have focused on the interactions between cancer and ECs, mostly using hydrogel
283 matrices. In general, these models have a gel-fluid interface that is lined with ECs to mimic a vessel wall, but their
284 geometry varies.

285 For example, the previously mentioned compartmentalized chip from (Zervantonakis et al., 2012) contains a
286 rectangular channel lined with ECs. The ECs are in contact with a cancer cell laden collagen I matrix, between the
287 micropillars that separate the compartments. This design has the advantage that imaging is relatively simple, due
288 to the well-defined tumor-vessel boundary, and later introduction of other cues, such as growth factors, is
289 possible.

290 More *in vivo* like cylindrical vessels have also been made, by patterning cylindrical channels in a cancer cell
291 laden collagen I gel, and lining them with ECs (Wong and Searson, 2014). Wang et al. further developed this type
292 of model and also incorporated a BM model, by patterning the cylindrical channel with a polysaccharide
293 microtube (Wang et al., 2015b). Although the shape of these models is more physiologically relevant,
294 quantification and imaging is more challenging.

295 Even more *in vivo* like vessels have also been made, by relying on EC self-assembly, provided that the right
296 cues are present in the chip. Lee et al. used a multi-compartmentalized chip to drive human umbilical vein
297 endothelial cells (HUVECs) to differentiate and self-assemble into a blood vessel inside a fibrin gel, a matrix
298 material normally involved in wound healing (Lee et al., 2014). Nearby compartments were seeded with lung
299 fibroblasts to provide the growth factors to induce and direct HUVEC self-assembly. These models are inherently
300 more similar to *in vivo* vessels, but also make quantitative analysis more challenging, again illustrating the trade-
301 off between physiological relevance and ease of analysis.

302 Using the models from (Lee et al., 2014; Zervantonakis et al., 2012), the effects of tumor necrosis factor alpha
303 (TNF- α) on vessel wall permeability and invasion rate were observed live, for both breast cancer and
304 fibrosarcoma cells. Additionally, the model of (Wang et al., 2015b) was used to demonstrate the pro-invasion
305 effect of Hepatocyte Growth Factor (HGF) for liver cancer cells.

306 In other work, intravasation into lymphatic vessels was studied using a hybrid Transwell-microfluidic system
307 that resembled a membrane chip (Pisano et al., 2015). In this system, both luminal and transmural flow could be
308 controlled, and both flow types were shown to have a promoting effect on the intravasation of breast cancer cells.

309 The main power of these methods is that they enable live observation of intravasation dynamics, such that
310 other relevant microenvironmental factors can be systematically studied, down to the single-invasion event level.
311 For example, one could incorporate different ECM environments in the chips above, to facilitate research into the
312 effect of ECM properties on EC resistance to cancer cell invasion.

313 **Modeling the cancer cell-ECM interactions**

314 Injectable hydrogels, mainly collagen I and Matrigel, a type of reconstituted BM, are often used as 3D matrices to
315 support cell growth and migration in microfluidic devices (Huang et al., 2009; Shin et al., 2014; Truong et al.,
316 2016). Recently, self-standing matrix layers, such as electrospun matrices, in a membrane chip have been
317 developed as an alternative (Eslami Amirabadi et al., 2017). These matrices offer more mechanical stability
318 compared to the hydrogels. When modeling cancer cell-ECM interactions in such CoC devices, the primary read-
319 out is usually the effect of the matrix composition on cancer invasion. For example, several studies compared
320 various ECM compositions between Matrigel, collagen I, and a mixture of both, to find the most appropriate
321 matrix to study cancer invasion (Anguiano et al., 2017; Huang et al., 2009; Sung et al., 2011; Truong et al., 2016).
322 Sung et al., using a Y chip, observed that non-invasive epithelial cancer cells require the mixture of the both gels
323 to grow in 3D clusters and transition to an invasive phenotype (Sung et al., 2011). In another study, focused on
324 the cancer cell heterogeneity in breast cancer, Shin et al. used a compartmentalized chip. They observed that
325 MCF-7 cells, an epithelial-like non-invasive cancer cell line, only follow the invasion path of MDA-MB-231
326 cells, a highly invasive cancer cell line, when grown in Matrigel, but not when grown in collagen I (Shin et al.,
327 2014). In a different study, Han et al. used a compartmentalized chip to create an assembly comparable to the *in*

328 *vivo* structure by aligning collagen fibers perpendicularly to a neighboring Matrigel layer (Figure 1D). They
329 observed that this heterogeneous interface makes the cells orient along the collagen fibers and invade into the
330 Matrigel layer, whereas cells in a homogeneous interface did not invade the Matrigel (Han et al., 2016).

331 The CoC community has also devoted significant attention to visualizing ECM remodeling, for which different
332 microscopy techniques can be used, such as second harmonic generation (SHG) (Drifka et al., 2013; Gioiella et
333 al., 2016; Huang et al., 2009; Sung et al., 2011), fluorescence (Shin et al., 2014; Sung et al., 2011), phase contrast
334 (Han et al., 2016; Shin et al., 2014) and scanning electron microscopy (Chaw et al., 2007). For instance, Wong et
335 al. used a lumen chip to image the formation of ECM microtracks that cancer cells create towards blood vessels
336 using phase contrast and fluorescence microscopy (Wong and Searson, 2014). In the previously mentioned work
337 by Sung et al., researchers studied the individual roles of cancer cells and fibroblasts in matrix remodeling using
338 SHG microscopy (Sung et al., 2011).

339 Only a few CoC publications have studied the relationship between the mechanical properties of the ECM and
340 cancer cell invasion. For example, Wong et al. suggest that stiffness and pore size in the ECM can be optimized to
341 enhance invasion by using a lower collagen concentration in dense matrices (Wong and Searson, 2014). A reverse
342 strategy, e.g. reinforcing the weakened ECM by artificial materials, can be a therapeutic approach to prevent
343 cancer invasion, especially in early stages of metastasis, reviewed in (Chen et al., 2017).

344 Current CoC platforms have helped us understand how ECM composition and its structure can affect cancer
345 cell invasion by visualizing matrix remodeling with different imaging techniques. In spite of this progress, CoC
346 models have much more potential to unravel cell-matrix interactions during cancer invasion, as we discuss below.

347 **Modeling mechanical cues in the tumor**

348 Interstitial fluid pressure and flow

349 Similarly to ECM-focused studies, lumen and compartmentalized chips have been predominantly used to
350 investigate the effects of IFP. These CoC approaches enabled, for the first time, to directly observe the response
351 of cancer cells to IFP, and to the interstitial fluid flow (IFF) that is caused by IFP gradients.

352 In a lumen chip, human MDA-MB-231 breast cancer cells grown as cell aggregates in collagen I could
353 reproducibly be subjected to an IFP gradient, with high pressure at the base of the aggregates and low pressure at
354 the tip, and vice versa (Tien et al., 2012). The authors measured invasion from the cell aggregate tips as illustrated
355 in Figure 3L, and showed that high IFP at the base decreased the invasiveness of the cell aggregate, whereas low
356 IFP at the base increased invasiveness. This invasion against a pressure gradient was also observed in the HepG2
357 and HLE liver cancer cell lines, using a collagen I matrix in a compartmentalized chip (Kalchman et al., 2013).
358 These studies indicate that cancer cells of different types tend to invade towards regions of higher pressure, such
359 as intratumoral blood vessels, to potentially metastasize. Interestingly, increased IFF from the tumor base to its
360 edge, seems to inhibit invasion from the tumor margin, indicating that invasion towards intratumoral blood

361 vessels might be the dominant mechanism for metastasis *in vivo*. By combining the model from (Tien et al., 2012)
362 with other analyses, such as Western blotting and qPCR, both mesenchymal markers, such as Snail and vimentin,
363 and the epithelial markers E-cadherin and keratin-8 were found to be upregulated under the invasion inducing IFP
364 gradient (Figure 3G,O) (Piotrowski-Daspit et al., 2016). In this condition, cancer cells invaded collectively against
365 the imposed IFP gradient, explaining the upregulated epithelial markers related to cell-cell contact. The
366 upregulation of EMT markers indicates that mesenchymal properties, typical for aggressive single cell migration,
367 are also necessary for the observed collective invasion.

368 In contrast to cancer cell aggregates, isolated cancer cells exhibited both up- and downstream migration when
369 subjected to IFF in a compartmentalized chip, and these migration patterns depended on the cell density
370 (Polacheck et al., 2011). This dependence could be explained by a competition between tensional cues from ECM
371 adhesions that induce upstream migration and autologous chemotaxis, which induces downstream migration. In
372 the latter case, an isolated cell is attracted to its own growth factors being carried downstream the IFF (Polacheck
373 et al., 2014). This local chemotactic gradient disappeared when cell numbers were increased, leading to more
374 upstream cell migration driven by the competing tensional cues. In other work, the different cellular
375 subpopulations that migrate either upstream or downstream could be identified by applying single cell tracking
376 inside compartmentalized chips under IF (Haessler et al., 2012). Moreover, a relationship between IFF and the
377 migration mode of cancer cells was found: when subjected to IFF, an increased number of cells exhibited
378 amoeboid migration, with fewer exhibiting mesenchymal migration (Huang et al., 2015; Box1), indicating that
379 isolated cancer cells might be driven towards a less mesenchymal phenotype, as opposed to cell aggregates. These
380 results imply that isolated cancer cells migrate, and thus metastasize, in different ways from cancer cell
381 aggregates. Although the relevance of single versus collective invasion is not completely clear, insights in the
382 mechanisms that underlie these types of invasion directed by IFP gradients could lead to more targeted
383 therapeutic approaches to prevent metastasis.

384 Mechanical tissue deformation

385 To our knowledge, only two CoC-based reports on the integration of physiological mechanical tissue deformation
386 have been published. Huang et al. studied ~~on~~ the interaction between fibroblasts and lung cancer cells in a
387 compartmentalized microfluidic chip, in which cancer cells were supplied with conditioned growth medium from
388 the fibroblast-containing chamber (Huang et al., 2013). By periodically stretching the fibroblast culture surface,
389 which mimicked the tensile strain lungs are subjected to during breathing cycles, the migration speed of the lung
390 cancer cells was significantly reduced. In recent work, non-small-cell lung cancer cells were included in a lung-
391 on-a-chip organ model that included both the epithelial cells layer, endothelial cell layer, and physiological
392 periodic strain (Hassell et al., 2017). Reduced invasion was observed in the dynamically stretched versus the static
393 samples, and the development of therapeutic resistance to tyrosine kinase inhibitor was observed in the dynamic

394 but not the static case. These works indicate that mechanical deformation can affect both cancer cell invasion and
395 therapeutic resistance.

396 The future of cancer-on-a-chip technology

397 As discussed in the previous sections, CoC approaches have been used to answer many questions about the
398 influence of the TME on cancer metastasis, but they have also generated new questions and opened up new
399 avenues of research. Here, we take a closer look at these questions and possible research directions. To tackle
400 these questions, researchers must choose the most appropriate chip design. For this purpose, we provide an
401 overview of CoC literature in the Supplementary table.

402 Most biochemical cue-oriented CoC studies have focused on oxygen, and some analyzed acidity and lactate
403 levels. Such research has indicated that aerotaxis is a relevant mechanism in cancer cell migration, and that acid
404 and lactate gradients play a role in directing cancer cell invasion. Our understanding of these effects is far from
405 complete, but the CoC methods discussed here are promising tools to investigate the effects of these and possibly
406 other biochemical gradients on cancer cells. Importantly, the contributions of these biochemical cues should be
407 evaluated in combination with different matrices and TME cell types, as we have seen that many of these effects
408 are influenced by TME factors, and not only by the cancer cells. A striking example is how hypoxia can both
409 directly induce invasion, but can also indirectly activate CAFs and MMPs to drive the ECM remodeling that
410 facilitates invasion.

411 Many kinds of cell-cell interactions have been studied in CoC devices. In the near future, they could be applied
412 to obtain additional insight in the mechanisms underlying the recruitment and activation of both CAFs and TAMs.
413 Moreover, the role of the M1/M2 phenotype of TAMs, the relevance of CAF subpopulations, or the extent to
414 which CAFs influence other stromal cells could be studied. Other possible experiments could be tailored towards
415 investigating the relatively new concept of angiocrine signaling and study the interaction mechanisms between
416 endothelial and cancer cells. Similarly, the relevance of intravasation into lymphatic vessels should be
417 investigated in more detail.

418 At this point, it is important to note that the list of different TME cell types discussed here is by no means
419 exhaustive; many more cell types, such as mesenchymal stem cells (Ma et al., 2012), natural killer cells (Ayuso et
420 al., 2016), dendritic cells (Parlato et al., 2017), and adipocytes play a role in invasion and intravasation, and their
421 roles could also be (or are being) studied in a CoC setting. The main challenge, however, is that the relative
422 contribution of an individual cell type is difficult to evaluate, as many can interact with each other and
423 synergistically activate the cancer cells. Future CoC work should therefore focus on understanding and evaluating
424 these types of cell-cell interactions.

425 The ECM has been studied to some extent in CoC systems, mainly focusing on the effect of ECM changes
426 during invasion. In future work, CoC models could be used to further increase our understanding of how the

427 mechanical properties and architecture of both the ECM and the BM affect invasion. This could be enabled by
428 patterning ECM and BM with different (mechanical) properties on a chip that facilitates control over cues, such as
429 chemotactic gradients and the cell types involved in matrix remodeling. By also varying the matrix composition,
430 more insight could be generated into the role of different ECM constituents in directing cellular behavior.

431 The CoC work on mechanical cues has mostly focused on interstitial pressure and flow as drivers of cancer
432 cell migration. The literature reviewed here demonstrates how the integration of more conventional read-outs
433 could lead to novel mechanistic insights, such as the competition between autologous chemotaxis and matrix-
434 mediated cancer cell migration. However, the integration of organ-level mechanical cues in CoC systems is
435 clearly still in its infancy. Most CoC devices are still relatively static, while many organs, such as the lung, colon,
436 and stomach, are highly dynamic. Here, the CoC field can learn from the broader field of organ-on-chip, in which
437 this type of mechanical cues have been integrated in many different organ models, reviewed in (Ingber, 2016).

438 We have seen that CoC models are an enabling technology for quantitative analysis of the roles of the different
439 TME cues in metastasis. However, evaluating the synergy between these cues in CoC chips, with the added
440 complexity of *in vivo* like cross-talk, is still a major challenge. Here, the field of CoC could benefit from more
441 advanced theoretical modeling, which could lead to extremely powerful approaches to study the TME and cancer
442 metastasis.

443 Conclusion

444 We have highlighted how different cues from the TME can affect the onset of metastasis, and we have reviewed
445 the most recent CoC developments showing how these models can help decipher the complex interplay within
446 and between the cancer cells and the TME. Furthermore, we have highlighted outstanding challenges for which
447 these promising technologies could be used. In a much broader perspective, the technologies developed for CoC
448 models are not limited to studying cancer invasion and the TME alone. Here, we focused on the onset of
449 metastasis, but CoC technology can be, and is, applied to study other steps in the process, such as extravasation
450 (Jeon et al., 2015). Whether used to study the full metastatic cascade or its onset alone, CoC technology has the
451 potential to reduce our reliance on animal models as a complementary research tool. Beyond generating
452 mechanistic insight in the metastatic cascade, CoC models could be combined with clinical material to investigate
453 patient-specific cancer progression. This could drastically change the way we can test drug efficacy, or even
454 develop new therapies to specifically prevent metastasis.

455 Acknowledgements

456 We would like to thank Dr. Katarina Wolf and Dr. Jean-Philippe Frimat for their valuable opinions and ideas.

457 Competing interests

458 The authors declare no competing or financial interests.

459 References

- 460 **Acosta, M. a, Jiang, X., Huang, P.-K., Cutler, K. B., Grant, C. S., Walker, G. M. and Gamcsik, M. P.** (2014). A microfluidic device to study
461 cancer metastasis under chronic and intermittent hypoxia. *Biomicrofluidics* **8**, 54117.
- 462 **Alemaný-Ribes, M. and Semino, C. E.** (2014). Bioengineering 3D environments for cancer models. *Adv. Drug Deliv. Rev.* **79–80**, 40–49.
- 463 **Anguiano, M., Castilla, C., Mařka, M., Ederra, C., Peláez, R., Morales, X., Muñoz-Arrieta, G., Mujika, M., Kozubek, M., Muñoz-Barrutia,**
464 **A., et al.** (2017). Characterization of three-dimensional cancer cell migration in mixed collagen-Matrigel scaffolds using
465 microfluidics and image analysis. *PLoS One* **12**, e0171417.
- 466 **Ayuso, J. M., Virumbrales-Muñoz, M., Lacueva, A., Lanuza, P. M., Checa-Chavarria, E., Botella, P., Fernández, E., Doblare, M., Allison, S.**
467 **J., Phillips, R. M., et al.** (2016). Development and characterization of a microfluidic model of the tumour microenvironment. *Sci.*
468 *Rep.* **6**, 36086.
- 469 **Bai, J., Adriani, G., Dang, T., Tu, T., Penny, H. L., Wong, S., Kamm, R. D. and Thiery, J.-P.** (2015). Contact-dependent carcinoma aggregate
470 dispersion by M2a macrophages via ICAM-1 and β 2 integrin interactions. *Oncotarget* **6**, 25295–25307.
- 471 **Balkwill, F. and Mantovani, A.** (2001). Inflammation and cancer: back to Virchow? *Lancet* **357**, 539–545.
- 472 **Belgiovine, C., D’Incalci, M., Allavena, P. and Frapolli, R.** (2016). Tumor-associated macrophages and anti-tumor therapies: complex
473 links. *Cell. Mol. Life Sci.* **73**, 2411–2424.
- 474 **Bhowmick, N. A., Neilson, E. G. and Moses, H. L.** (2004). Stromal fibroblasts in cancer initiation and progression. *Nature* **432**, 332–337.
- 475 **Bierie, B. and Moses, H. L.** (2006). Tumour microenvironment: TGF β : the molecular Jekyll and Hyde of cancer. *Nat. Rev. Cancer* **6**, 506–
476 520.
- 477 **Bischel, L. L., Beebe, D. J. and Sung, K. E.** (2015). Microfluidic model of ductal carcinoma in situ with 3D, organotypic structure. *BMC*
478 *Cancer* **15**, 12.
- 479 **Bissell, M. J., Hall, H. G. and Parry, G.** (1982). How does the extracellular matrix direct gene expression? *J. Theor. Biol.* **99**, 31–68.
- 480 **Buhtoiarov, I. N., Sondel, P. M., Wigginton, J. M., Buhtoiarova, T. N., Yanke, E. M., Mahvi, D. A. and Rakhmilevich, A. L.** (2011). Anti-
481 tumour synergy of cytotoxic chemotherapy and anti-CD40 plus CpG-ODN immunotherapy through repolarization of tumour-
482 associated macrophages. *Immunology* **132**, 226–239.
- 483 **Butcher, D. T., Alliston, T. and Weaver, V. M.** (2009). A tense situation: forcing tumour progression. *Nat. Rev. Cancer* **9**, 108–122.
- 484 **Butler, J. M., Kobayashi, H. and Rafii, S.** (2010). Instructive role of the vascular niche in promoting tumour growth and tissue repair by
485 angiocrine factors. *Nat. Rev. Cancer* **10**, 138–146.
- 486 **Cao, Z., Ding, B.-S., Guo, P., Lee, S. B., Butler, J. M., Casey, S. C., Simons, M., Tam, W., Felsher, D. W., Shido, K., et al.** (2014). Angiocrine
487 Factors Deployed by Tumor Vascular Niche Induce B Cell Lymphoma Invasiveness and Chemoresistance. *Cancer Cell* **25**, 350–365.
- 488 **Chang, C.-W., Cheng, Y.-J., Tu, M., Chen, Y.-H., Peng, C.-C., Liao, W.-H. and Tung, Y.-C.** (2014). A polydimethylsiloxane–polycarbonate
489 hybrid microfluidic device capable of generating perpendicular chemical and oxygen gradients for cell culture studies. *Lab Chip* **14**,
490 3762–3772.
- 491 **Chaw, K. C., Manimaran, M., Tay, F. E. H. and Swaminathan, S.** (2007). Matrigel coated polydimethylsiloxane based microfluidic devices
492 for studying metastatic and non-metastatic cancer cell invasion and migration. *Biomed. Microdevices* **9**, 597–602.

493 **Chen, Y.-A., King, A. D., Shih, H.-C., Peng, C.-C., Wu, C.-Y., Liao, W.-H. and Tung, Y.-C.** (2011). Generation of oxygen gradients in
494 microfluidic devices for cell culture using spatially confined chemical reactions. *Lab Chip* **11**, 3626.

495 **Chen, Q., Liu, G., Liu, S., Su, H., Wang, Y., Li, J. and Luo, C.** (2017). Remodeling the Tumor Microenvironment with Emerging
496 Nanotherapeutics. *Trends Pharmacol. Sci.* **39**, 59–74.

497 **Choi, S. Y. C., Lin, D., Gout, P. W., Collins, C. C., Xu, Y. and Wang, Y.** (2014). Lessons from patient-derived xenografts for better in vitro
498 modeling of human cancer. *Adv. Drug Deliv. Rev.* **79**, 222–237.

499 **Choi, Y., Hyun, E., Seo, J., Blundell, C., Kim, H. C., Lee, E., Lee, S. H., Moon, A., Moon, W. K. and Huh, D.** (2015). A microengineered
500 pathophysiological model of early-stage breast cancer. *Lab Chip* **15**, 3350–3357.

501 **Cirri, P. and Chiarugi, P.** (2012). Cancer-associated-fibroblasts and tumour cells: A diabolic liaison driving cancer progression. *Cancer*
502 *Metastasis Rev.* **31**, 195–208.

503 **Coussens, L. M. and Werb, Z.** (2002). Inflammation and cancer. *Nature* **420**, 860–867.

504 **Cox, T. R., Bird, D., Baker, A.-M., Barker, H. E., Ho, M. W.-Y., Lang, G. and Erler, J. T.** (2013). LOX-Mediated Collagen Crosslinking Is
505 Responsible for Fibrosis-Enhanced Metastasis. *Cancer Res.* **73**, 1721–1732.

506 **Darby, I. A. and Hewitson, T. D.** (2007). Fibroblast Differentiation in Wound Healing and Fibrosis. *Int. Rev. Cytol.* **257**, 143–179.

507 **Deryugina, E. I. and Quigley, J. P.** (2006). Matrix metalloproteinases and tumor metastasis. *Cancer Metastasis Rev.* **25**, 9–34.

508 **Dijkgraaf, E. M., Heusinkveld, M., Tummers, B., Vogelpoel, L. T. C., Goedemans, R., Jha, V., Nortier, J. W. R., Welters, M. J. P., Kroep, J.**
509 **R. and Van Der Burg, S. H.** (2013). Chemotherapy alters monocyte differentiation to favor generation of cancer-supporting m2
510 macrophages in the tumor microenvironment. *Cancer Res.* **73**, 2480–2492.

511 **Drifka, C. R., Eliceiri, K. W., Weber, S. M. and Kao, W. J.** (2013). A bioengineered heterotypic stroma–cancer microenvironment model to
512 study pancreatic ductal adenocarcinoma. *Lab Chip* **13**, 3965–3975.

513 **Egeblad, M., Rasch, M. G. and Weaver, V. M.** (2010). Dynamic interplay between the collagen scaffold and tumor evolution. *Curr. Opin.*
514 *Cell Biol.* **22**, 697–706.

515 **Eslami Amirabadi, H., SahebAli, S., Frimat, J. P., Luttge, R. and den Toonder, J. M. J.** (2017). A novel method to understand tumor cell
516 invasion: integrating extracellular matrix mimicking layers in microfluidic chips by “selective curing.” *Biomed. Microdevices* **19**, 92.

517 **Estrella, V., Chen, T., Lloyd, M., Wojtkowiak, J., Cornell, H. H., Ibrahim-Hashim, A., Bailey, K., Balagurunathan, Y., Rothberg, J. M.,**
518 **Sloane, B. F., et al.** (2013). Acidity Generated by the Tumor Microenvironment Drives Local Invasion. *Cancer Res.* **73**, 1524–1535.

519 **Frantz, C., Stewart, K. M. and Weaver, V. M.** (2010). The extracellular matrix at a glance. *J. Cell Sci.* **123**, 4195–4200.

520 **Friedl, P. and Alexander, S.** (2011). Cancer invasion and the microenvironment: Plasticity and reciprocity. *Cell* **147**, 992–1009.

521 **Friedl, P. and Wolf, K.** (2008). Tube Travel: The Role of Proteases in Individual and Collective Cancer Cell Invasion. *Cancer Res.* **68**, 7247–
522 7249.

523 **Funamoto, K., Zervantonakis, I. K., Liu, Y., Ochs, C. J., Kim, C. and Kamm, R. D.** (2012). A novel microfluidic platform for high-resolution
524 imaging of a three-dimensional cell culture under a controlled hypoxic environment. *Lab Chip* **12**, 4855–4863.

525 **Gatenby, R. A., Gawlinski, E. T., Gmitro, A. F., Kaylor, B. and Gillies, R. J.** (2006). Acid-Mediated Tumor Invasion: a Multidisciplinary
526 Study. *Cancer Res.* **66**, 5216–5223.

527 **Ghiabi, P., Jiang, J., Pasquier, J., Maleki, M., Abu-Kaoud, N., Rafii, S. and Rafii, A.** (2014). Endothelial Cells Provide a Notch-Dependent
528 Pro-Tumoral Niche for Enhancing Breast Cancer Survival, Stemness and Pro-Metastatic Properties. *PLoS One* **9**, e112424.

529 **Gioiella, F., Urciuolo, F., Imparato, G., Brancato, V. and Netti, P. A.** (2016). An Engineered Breast Cancer Model on a Chip to Replicate
530 ECM-Activation In Vitro during Tumor Progression. *Adv. Healthc. Mater.* **5**, 3074–3084.

531 **Goetze, K., Walenta, S., Ksiazkiewicz, M., Kunz-Schughart, L. A. and Mueller-Klieser, W.** (2011). Lactate enhances motility of tumor cells

532 and inhibits monocyte migration and cytokine release. *Int. J. Oncol.* **39**, 453–63.

533 **Haessler, U., Teo, J. C. M., Foretay, D., Renaud, P. and Swartz, M. a.** (2012). Migration dynamics of breast cancer cells in a tunable 3D
534 interstitial flow chamber. *Integr. Biol.* **4**, 401–409.

535 **Han, W., Chen, S., Yuan, W., Fan, Q., Tian, J., Wang, X., Chen, L., Zhang, X., Wei, W., Liu, R., et al.** (2016). Oriented collagen fibers direct
536 tumor cell intravasation. *Proc. Natl. Acad. Sci.* **113**, 11208–11213.

537 **Hanahan, D. and Weinberg, R. A.** (2011). Hallmarks of cancer: The next generation. *Cell* **144**, 646–674.

538 **Hassell, B. A., Goyal, G., Lee, E., Sontheimer-Phelps, A., Levy, O., Chen, C. S. and Ingber, D. E.** (2017). Human Organ Chip Models
539 Recapitulate Orthotopic Lung Cancer Growth, Therapeutic Responses, and Tumor Dormancy In Vitro. *Cell Rep.* **21**, 508–516.

540 **Hendricks, P., Diaz, F. J., Schmitt, S., Sitta Sittampalam, G. and Nirmalanandhan, V. S.** (2012). Effects of respiratory mechanical forces on
541 the pharmacological response of lung cancer cells to chemotherapeutic agents. *Fundam. Clin. Pharmacol.* **26**, 632–643.

542 **Hompland, T., Lund, K. V., Ellingsen, C., Kristensen, G. B. and Rofstad, E. K.** (2014). Peritumoral interstitial fluid flow velocity predicts
543 survival in cervical carcinoma. *Radiother. Oncol.* **113**, 132–138.

544 **Hsu, T.-H., Xiao, J.-L., Tsao, Y.-W., Kao, Y.-L., Huang, S.-H., Liao, W.-Y. and Lee, C.-H.** (2011). Analysis of the paracrine loop between
545 cancer cells and fibroblasts using a microfluidic chip. *Lab Chip* **11**, 1808–1814.

546 **Hu, W., Li, X., Zhang, C., Yang, Y., Jiang, J. and Wu, C.** (2016). Tumor-associated macrophages in cancers. *Clin. Transl. Oncol.* **18**, 251–258.

547 **Huang, C. P., Lu, J., Seon, H., Lee, A. P., Flanagan, L. a, Kim, H.-Y., Putnam, A. J. and Jeon, N. L.** (2009). Engineering microscale cellular
548 niches for three-dimensional multicellular co-cultures. *Lab Chip* **9**, 1740–1748.

549 **Huang, J.-W., Pan, H.-J., Yao, W.-Y., Tsao, Y.-W., Liao, W.-Y., Wu, C.-W., Tung, Y.-C. and Lee, C.-H.** (2013). Interaction between lung
550 cancer cell and myofibroblast influenced by cyclic tensile strain. *Lab Chip* **13**, 1114–1120.

551 **Huang, Y. L., Tung, C.-K., Zheng, A., Kim, B. J. and Wu, M.** (2015). Interstitial flows promote amoeboid over mesenchymal motility of
552 breast cancer cells revealed by a three dimensional microfluidic model. *Integr. Biol.* **7**, 1402–1411.

553 **Hynes, R. O.** (2009). The Extracellular Matrix: Not Just Pretty Fibrils. *Science* **326**, 1216–1219.

554 **Ingber, D. E.** (2016). Reverse Engineering Human Pathophysiology with Organs-on-Chips. *Cell* **164**, 1105–1109.

555 **Jeon, J. S., Bersini, S., Gilardi, M., Dubini, G., Charest, J. L., Moretti, M. and Kamm, R. D.** (2015). Human 3D vascularized organotypic
556 microfluidic assays to study breast cancer cell extravasation. *Proc. Natl. Acad. Sci.* **112**, 214–219.

557 **Joyce, J. A. and Pollard, J. W.** (2009). Microenvironmental regulation of metastasis. *Nat. Rev. Cancer* **9**, 239–252.

558 **Kalchman, J., Fujioka, S., Chung, S., Kikkawa, Y., Mitaka, T., Kamm, R. D., Tanishita, K. and Sudo, R.** (2013). A three-dimensional
559 microfluidic tumor cell migration assay to screen the effect of anti-migratory drugs and interstitial flow. *Microfluid. Nanofluidics* **14**,
560 969–981.

561 **Kalluri, R. and Zeisberg, M.** (2006). Fibroblasts in cancer. *Nat. Rev. Cancer* **6**, 392–401.

562 **Kato, Y., Ozawa, S., Miyamoto, C., Maehata, Y., Suzuki, A., Maeda, T. and Baba, Y.** (2013). Acidic extracellular microenvironment and
563 cancer. *Cancer Cell Int.* **13**, 89.

564 **Koumoutsakos, P., Pivkin, I. and Milde, F.** (2013). The Fluid Mechanics of Cancer and Its Therapy. *Annu. Rev. Fluid Mech.* **45**, 325–355.

565 **Kumar, S. and Weaver, V. M.** (2009). Mechanics, malignancy, and metastasis: The force journey of a tumor cell. *Cancer Metastasis Rev.*
566 **28**, 113–127.

567 **Kuzet, S. E. and Gaggioli, C.** (2016). Fibroblast activation in cancer: when seed fertilizes soil. *Cell Tissue Res.* **365**, 607–619.

568 **Lee, H., Park, W., Ryu, H. and Jeon, N. L.** (2014). A microfluidic platform for quantitative analysis of cancer angiogenesis and
569 intravasation. *Biomicrofluidics* **8**, 54102.

570 **Lee, E., Song, H.-H. G. and Chen, C. S.** (2016). Biomimetic on-a-chip platforms for studying cancer metastasis. *Curr. Opin. Chem. Eng.* **11**,

571 20–27.

572 **Lehmann, S., te Boekhorst, V., Odenthal, J., Bianchi, R., van Helvert, S., Ikenberg, K., Ilina, O., Stoma, S., Xandry, J., Jiang, L., et al.**

573 (2017). Hypoxia Induces a HIF-1-Dependent Transition from Collective-to-Amoeboid Dissemination in Epithelial Cancer Cells. *Curr.*

574 *Biol.* **27**, 392–400.

575 **Leight, J. L., Wozniak, M. a., Chen, S., Lynch, M. L. and Chen, C. S.** (2012). Matrix rigidity regulates a switch between TGF- 1-induced

576 apoptosis and epithelial-mesenchymal transition. *Mol. Biol. Cell* **23**, 781–791.

577 **Lewis, C. E. and Pollard, J. W.** (2006). Distinct Role of Macrophages in Different Tumor Microenvironments. *Cancer Res.* **66**, 605–612.

578 **Li, J., Jia, Z., Kong, J., Zhang, F., Fang, S., Li, X., Li, W., Yang, X., Luo, Y., Lin, B., et al.** (2016). Carcinoma-associated fibroblasts lead the

579 invasion of salivary gland adenoid cystic carcinoma cells by creating an invasive track. *PLoS One* **11**, 1–15.

580 **Lin, E. Y., Li, J.-F., Gnatovskiy, L., Deng, Y., Zhu, L., Grzesik, D. A., Qian, H., Xue, X. -n. and Pollard, J. W.** (2006). Macrophages Regulate

581 the Angiogenic Switch in a Mouse Model of Breast Cancer. *Cancer Res.* **66**, 11238–11246.

582 **Liu, T., Lin, B., Qin, J., Toh, Y.-C., Zhang, C., Zhang, J., Khong, Y. M., Chang, S., Samper, V. D., van Noort, D., et al.** (2007). Carcinoma-

583 associated fibroblasts promoted tumor spheroid invasion on a microfluidic 3D co-culture device. *Lab Chip* **7**, 302–309.

584 **Lu, P., Weaver, V. M. and Werb, Z.** (2012). The extracellular matrix: A dynamic niche in cancer progression. *J. Cell Biol.* **196**, 395–406.

585 **Lynch, C. C. and Matrisian, L. M.** (2002). Matrix metalloproteinases in tumor-host cell communication. *Differentiation* **70**, 561–573.

586 **Ma, H., Liu, T., Qin, J. and Lin, B.** (2010). Characterization of the interaction between fibroblasts and tumor cells on a microfluidic co-

587 culture device. *Electrophoresis* **31**, 1599–1605.

588 **Ma, H., Zhang, M. and Qin, J.** (2012). Probing the role of mesenchymal stem cells in salivary gland cancer on biomimetic microdevices.

589 *Integr. Biol.* **4**, 522–530.

590 **Mantovani, A. and Allavena, P.** (2015). The interaction of anticancer therapies with tumor-associated macrophages. *J. Exp. Med.* **212**,

591 435–445.

592 **Mantovani, A. and Sica, A.** (2010). Macrophages, innate immunity and cancer: balance, tolerance, and diversity. *Curr. Opin. Immunol.* **22**,

593 231–237.

594 **Mantovani, A., Sozzani, S., Locati, M., Allavena, P. and Sica, A.** (2002). Macrophage polarization: tumor-associated macrophages as a

595 paradigm for polarized M2 mononuclear phagocytes. *Trends Immunol.* **23**, 549–555.

596 **Mantovani, A., Allavena, P., Sica, A. and Balkwill, F.** (2008). Cancer-related inflammation. *Nature* **454**, 436–444.

597 **Mosser, D. M. and Edwards, J. P.** (2008). Exploring the full spectrum of macrophage activation. *Nat. Rev. Immunol.* **8**, 958–969.

598 **Nagy, J., Chang, S.-H., Shih, S.-C., Dvorak, A. and Dvorak, H.** (2010). Heterogeneity of the Tumor Vasculature. *Semin. Thromb. Hemost.*

599 **36**, 321–331.

600 **Oppegard, S. C. and Eddington, D. T.** (2013). A microfabricated platform for establishing oxygen gradients in 3-D constructs. *Biomed.*

601 *Microdevices* **15**, 407–414.

602 **Ostuni, R., Kratochvill, F., Murray, P. J. and Natoli, G.** (2015). Macrophages and cancer: from mechanisms to therapeutic implications.

603 *Trends Immunol.* **36**, 229–239.

604 **Parlato, S., De Ninno, A., Molfetta, R., Toschi, E., Salerno, D., Mencattini, A., Romagnoli, G., Fragale, A., Roccazzello, L., Buoncervello,**

605 **M., et al.** (2017). 3D Microfluidic model for evaluating immunotherapy efficacy by tracking dendritic cell behaviour toward tumor

606 cells. *Sci. Rep.* **7**, 1093.

607 **Parsonage, G., Filer, A. D., Haworth, O., Nash, G. B., Rainger, G. E., Salmon, M. and Buckley, C. D.** (2005). A stromal address code

608 defined by fibroblasts. *Trends Immunol.* **26**, 150–156.

609 **Paszek, M. J. and Weaver, V. M.** (2004). The tension mounts: Mechanics meets morphogenesis and malignancy. *J. Mammary Gland Biol.*

610 *Neoplasia* **9**, 325–342.

611 **Paszek, M. J., Zahir, N., Johnson, K. R., Lakins, J. N., Rozenberg, G. I., Gefen, A., Reinhart-King, C. A., Margulies, S. S., Dembo, M.,**
612 **Boettiger, D., et al.** (2005). Tensional homeostasis and the malignant phenotype. *Cancer Cell* **8**, 241–254.

613 **Piotrowski-Daspiet, A. S., Tien, J. and Nelson, C. M.** (2016). Interstitial fluid pressure regulates collective invasion in engineered human
614 breast tumors via Snail, vimentin, and E-cadherin. *Integr. Biol.* **8**, 319–331.

615 **Pisano, M., Triacca, V., Barbee, K. A. and Swartz, M. A.** (2015). An in vitro model of the tumor-lymphatic microenvironment with
616 simultaneous transendothelial and luminal flows reveals mechanisms of flow enhanced invasion. *Integr. Biol.* **7**, 525–533.

617 **Polacheck, W. J., Charest, J. L. and Kamm, R. D.** (2011). Interstitial flow influences direction of tumor cell migration through competing
618 mechanisms. *Proc. Natl. Acad. Sci.* **108**, 11115–11120.

619 **Polacheck, W. J., German, A. E., Mammoto, A., Ingber, D. E. and Kamm, R. D.** (2014). Mechanotransduction of fluid stresses governs 3D
620 cell migration. *Proc. Natl. Acad. Sci.* **111**, 2447–2452.

621 **Portillo-Lara, R. and Annabi, N.** (2016). Microengineered cancer-on-a-chip platforms to study the metastatic microenvironment. *Lab Chip*
622 **16**, 4063–4081.

623 **Räsänen, K. and Vaheri, A.** (2010). Activation of fibroblasts in cancer stroma. *Exp. Cell Res.* **316**, 2713–2722.

624 **Rofstad, E. K., Mathiesen, B., Kindem, K. and Galappathi, K.** (2006). Acidic Extracellular pH Promotes Experimental Metastasis of Human
625 Melanoma Cells in Athymic Nude Mice. *Cancer Res.* **66**, 6699–6707.

626 **Rolny, C., Mazzone, M., Tugues, S., Laoui, D., Johansson, I., Coulon, C., Squadrito, M. L., Segura, I., Li, X., Knevels, E., et al.** (2011). HRG
627 inhibits tumor growth and metastasis by inducing macrophage polarization and vessel normalization through downregulation of
628 PlGF. *Cancer Cell* **19**, 31–44.

629 **Sangaletti, S., Stoppacciaro, A., Guiducci, C., Torrisi, M. R. and Colombo, M. P.** (2003). Leukocyte, Rather than Tumor-produced SPARC,
630 Determines Stroma and Collagen Type IV Deposition in Mammary Carcinoma. *J. Exp. Med.* **198**, 1475–1485.

631 **Semenza, G. L.** (2003). Targeting HIF-1 for cancer therapy. *Nat. Rev. Cancer* **3**, 721–732.

632 **Semenza, G. L.** (2013). Cancer–stromal cell interactions mediated by hypoxia-inducible factors promote angiogenesis, lymphangiogenesis,
633 and metastasis. *Oncogene* **32**, 4057–4063.

634 **Semenza, G. L.** (2016). The hypoxic tumor microenvironment: A driving force for breast cancer progression. *Biochim. Biophys. Acta - Mol.*
635 *Cell Res.* **1863**, 382–391.

636 **Shieh, A. C. and Swartz, M. a** (2011). Regulation of tumor invasion by interstitial fluid flow. *Phys. Biol.* **8**, 15012.

637 **Shimoda, M., Mellody, K. T. and Orimo, A.** (2010). Carcinoma-associated fibroblasts are a rate-limiting determinant for tumour
638 progression. *Semin. Cell Dev. Biol.* **21**, 19–25.

639 **Shin, Y., Han, S., Chung, E. and Chung, S.** (2014). Intratumoral phenotypic heterogeneity as an encourager of cancer invasion. *Integr. Biol.*
640 **6**, 654–661.

641 **Sica, A., Larghi, P., Mancino, A., Rubino, L., Porta, C., Totaro, M. G., Rimoldi, M., Biswas, S. K., Allavena, P. and Mantovani, A.** (2008).
642 Macrophage polarization in tumour progression. *Semin. Cancer Biol.* **18**, 349–355.

643 **Sung, K. E., Yang, N., Pehlke, C., Keely, P. J., Eliceiri, K. W., Friedl, A. and Beebe, D. J.** (2011). Transition to invasion in breast cancer: a
644 microfluidic in vitro model enables examination of spatial and temporal effects. *Integr. Biol.* **3**, 439–450.

645 **Tao, L., Huang, G., Song, H., Chen, Y. and Chen, L.** (2017). Cancer associated fibroblasts: An essential role in the tumor microenvironment
646 (review). *Oncol. Lett.* **14**, 2611–2620.

647 **Tien, J., Truslow, J. G. and Nelson, C. M.** (2012). Modulation of Invasive Phenotype by Interstitial Pressure-Driven Convection in
648 Aggregates of Human Breast Cancer Cells. *PLoS One* **7**, e45191.

649 **Truong, D., Puleo, J., Llave, A., Mouneimne, G., Kamm, R. D. and Nikkhah, M.** (2016). Breast Cancer Cell Invasion into a Three
650 Dimensional Tumor-Stroma Microenvironment. *Sci. Rep.* **6**, 34094.

651 **Van Zijl, F., Krupitza, G. and Mikulits, W.** (2011). Initial steps of metastasis: Cell invasion and endothelial transmigration. *Mutat. Res. -*
652 *Rev. Mutat. Res.* **728**, 23–34.

653 **Vihinen, P. and Kähäri, V.-M.** (2002). Matrix metalloproteinases in cancer: Prognostic markers and therapeutic targets. *Int. J. Cancer* **99**,
654 157–166.

655 **Walsh, C. L., Babin, B. M., Kasinskas, R. W., Foster, J. A., McGarry, M. J. and Forbes, N. S.** (2009). A multipurpose microfluidic device
656 designed to mimic microenvironment gradients and develop targeted cancer therapeutics. *Lab Chip* **9**, 545–554.

657 **Wang, L., Liu, W., Wang, Y., Wang, J., Tu, Q., Liu, R. and Wang, J.** (2013). Construction of oxygen and chemical concentration gradients in
658 a single microfluidic device for studying tumor cell-drug interactions in a dynamic hypoxia microenvironment. *Lab Chip* **13**, 695–
659 705.

660 **Wang, Z., Liu, Z., Li, L. and Liang, Q.** (2015a). Investigation into the hypoxia-dependent cytotoxicity of anticancer drugs under oxygen
661 gradient in a microfluidic device. *Microfluid. Nanofluidics* **19**, 1271–1279.

662 **Wang, X.-Y., Pei, Y., Xie, M., Jin, Z., Xiao, Y., Wang, Y., Zhang, L., Li, Y. and Huang, W.** (2015b). An artificial blood vessel implanted three-
663 dimensional microsystem for modeling transvascular migration of tumor cells. *Lab Chip* **15**, 1178–1187.

664 **Weigelt, B., Ghajar, C. M. and Bissell, M. J.** (2014). The need for complex 3D culture models to unravel novel pathways and identify
665 accurate biomarkers in breast cancer. *Adv. Drug Deliv. Rev.* **69–70**, 42–51.

666 **Whitehead, J., Vignjevic, D., Fütterer, C., Beaurepaire, E., Robine, S. and Farge, E.** (2008). Mechanical factors activate β -catenin-
667 dependent oncogene expression in APC 1638N/+ mouse colon. *HFSP J.* **2**, 286–294.

668 **Whitesides, G. M.** (2006). The origins and the future of microfluidics. *Nature* **442**, 368–373.

669 **Wong, A. D. and Searson, P. C.** (2014). Live-Cell Imaging of Invasion and Intravasation in an Artificial Microvessel Platform. *Cancer Res.*
670 **74**, 4937–4945.

671 **Xia, Y. and Whitesides, G. M.** (1998). SOFT LITHOGRAPHY. *Annu. Rev. Mater. Sci.* **28**, 153–184.

672 **Xouri, G. and Christian, S.** (2010). Origin and function of tumor stroma fibroblasts. *Semin. Cell Dev. Biol.* **21**, 40–46.

673 **Xu, X.-D., Shao, S.-X., Cao, Y.-W., Yang, X.-C., Shi, H.-Q., Wang, Y.-L., Xue, S.-Y., Wang, X.-S. and Niu, H.-T.** (2015). The study of energy
674 metabolism in bladder cancer cells in co-culture conditions using a microfluidic chip. *Int. J. Clin. Exp. Med.* **8**, 12327–12336.

675 **Yahara, D., Yoshida, T., Enokida, Y. and Takahashi, E.** (2016). Directional Migration of MDA-MB-231 Cells Under Oxygen Concentration
676 Gradients. In *Advances in Experimental Medicine and Biology*, pp. 129–134.

677 **Yu, T., Guo, Z., Fan, H., Song, J., Liu, Y., Gao, Z. and Wang, Q.** (2016). Cancer-associated fibroblasts promote non-small cell lung cancer
678 cell invasion by upregulation of glucose-regulated protein 78 (GRP78) expression in an integrated bionic microfluidic device.
679 *Oncotarget* **7**, 25593–25603.

680 **Zervantonakis, I. K., Hughes-Alford, S. K., Charest, J. L., Condeelis, J. S., Gertler, F. B. and Kamm, R. D.** (2012). Three-dimensional
681 microfluidic model for tumor cell intravasation and endothelial barrier function. *Proc. Natl. Acad. Sci.* **109**, 13515–13520.

682 **Zhao, Y., Wang, D., Xu, T., Liu, P., Cao, Y., Wang, Y., Yang, X., Xu, X., Wang, X. and Niu, H.** (2015). Bladder cancer cells re-educate TAMs
683 through lactate shuttling in the microfluidic cancer microenvironment. *Oncotarget* **6**, 39196–39210.

684

Box 1. Glossary

Amoeboid migration: A mode of migration where cancer cells migrate with low cell-matrix interactions and a rounded, less protrusive morphology (Friedl and Alexander, 2011). This choice of migration depends on the cell type and the TME, and does not require EMT.

Angiocrine signaling: Signals produced by endothelial cells that can affect cancer cell behavior.

Angiogenesis: The process through which new blood vessels form in the TME, sprouting from existing vessels.

Basement membrane (BM): A type of pericellular matrix that is in close contact with epithelial tissue.

Cancer Associated Fibroblasts (CAFs): Activated fibroblasts in the TME, with extensive roles in cancer progression.

Epithelial to mesenchymal transition (EMT): The transition through which cells obtain a more migratory phenotype, with fewer cell-cell and more focal adhesion sites (Friedl and Alexander, 2011).

Extracellular matrix (ECM): The non-cellular fibrous regulatory support structure of most tissues. In this review, ECM solely refers to the collagen I rich interstitial matrix.

Extravasation: Describes cancer cells that leave the circulation by crossing the vessel wall to enter a metastatic niche.

Intravasation: Describes cancer cells crossing the vessel wall to enter the circulation.

Invasion: Describes cancer cells breaking through the basement membrane, and invading the stromal tissue surrounding the tumor.

Matrix Metalloproteinases (MMPs): A family of proteolytic enzymes capable of degrading the extracellular matrix, secreted by or membrane-tethered to cancer and stromal cells, reviewed in (Lynch and Matrisian, 2002).

Mesenchymal migration: A mode of migration in which cancer cells migrate with strong cell-matrix interactions and an elongated, more protrusive morphology (Friedl and Alexander, 2011). This choice of migration depends on the cell type and the TME, and generally requires EMT.

Microfluidic chip: Device that contains small channels, with cross-sectional dimensions typically below 1 mm. Different channel arrangements and control methods enable very accurate control of fluid flow, (shear) forces, and pressure, reviewed in (Whitesides, 2006).

Paracrine signaling: Signals produced by cells to induce changes in the cells in their microenvironment.

Solid stress: The stresses within the tumor resulting from high proliferation of cancer cells and ECM stiffening.

Spheroids: Spherical three dimensional aggregates composed of proliferating cancer cells.

Tumor Microenvironment (TME): The collection of everything in close proximity of cancer cells, comprised of biochemical signals, different cells, the extracellular matrix, and mechanical cues.

Tumor Associated Macrophages (TAMs): The most abundant immune cells in the TME.

Warburg effect: The difference in the metabolism between cancer cells and healthy cells. In almost all cancers, cells rely more on inefficient glycolysis, while healthy cells generally rely on pyruvate oxidation in the mitochondria.

Box 2. Cancer-on-a-chip

Cancer-on-a-chip (CoC) models are based on microfluidic chips with micrometer to millimeter-sized compartments and microchannels that enable controlled fluid transport. The compartments can be used to reproducibly create a niche in which “mini-tumors” can grow, develop and interact within their own specified microenvironment, similarly to human tumors, reviewed in (Lee et al., 2016; Portillo-Lara and Annabi, 2016). Because of their small size, the cellular and matrix composition, local biochemical gradients, and mechanical forces like shear and stretch, can be highly controlled. These compartments are optically accessible for live observation, as most chips are made from polydimethylsiloxane (PDMS) using soft lithography, reviewed in (Xia and Whitesides, 1998). PDMS is a soft, transparent silicone material that is permeable to gases, enabling O₂ and CO₂ equilibration. Additionally, all microfluidic devices work with small reagent volumes, which reduces the experimental costs.

Different types of CoC models exist, as detailed in Figure 2. They contain microfluidic compartments to culture cells, either on a flat substrate (in 2D chips), or in a 3D matrix (in lumen, compartmentalized, or Y chips), or in a double layer on a porous membrane (in membrane chips). Depending on their design, different cues from the TME can be modeled and accurately controlled in these chips. These properties make CoC devices an excellent tool for studying the interactions between cancer cells and their microenvironment.

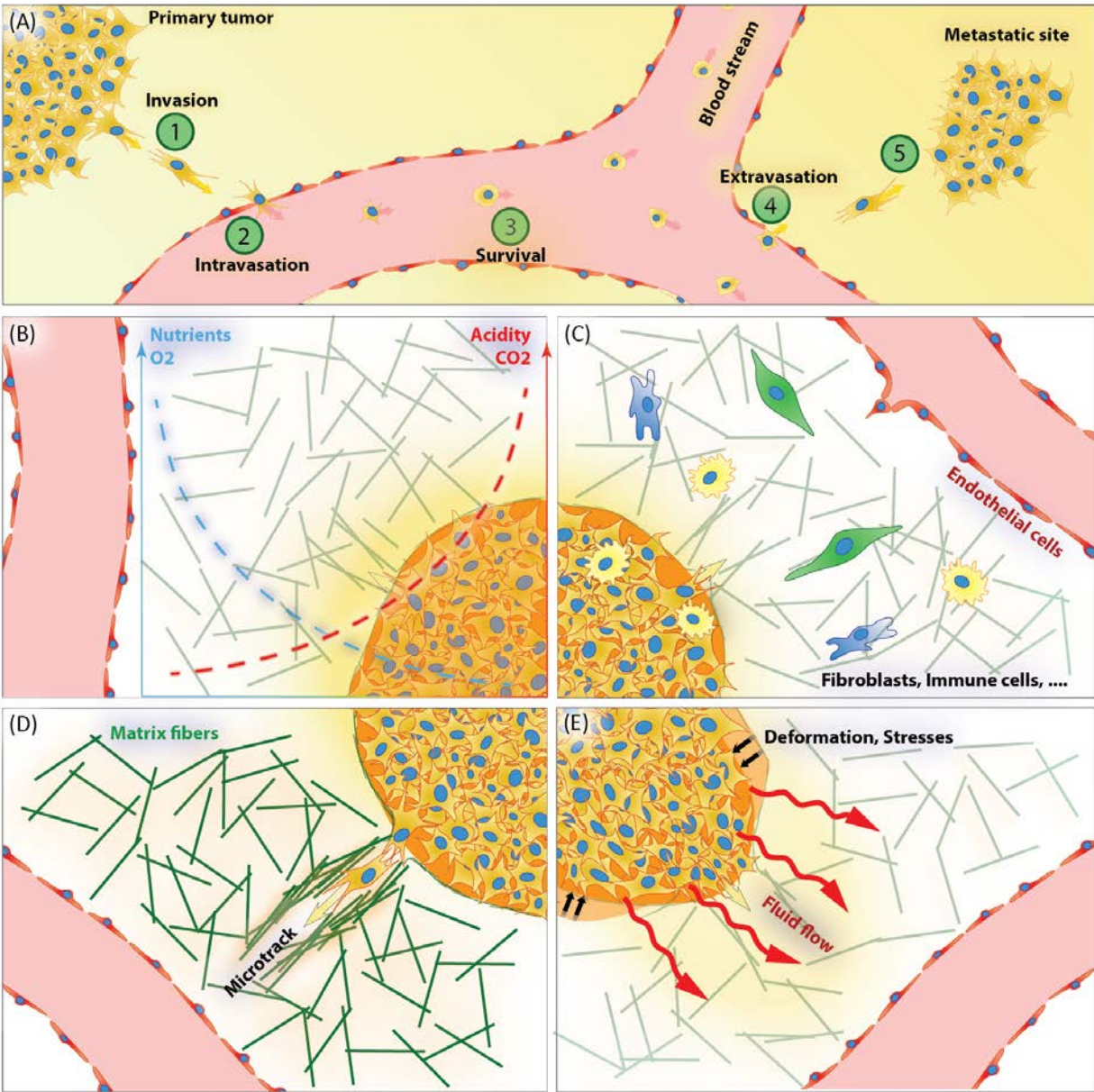


Figure 1 – Metastasis and the TME: (A) The five steps of metastasis; 1) Invasion; cancer cells escape from the primary tumor into the surrounding stroma. 2) Intravasation; cancer cells cross the vessel wall and enter the circulation. 3) Survival; cancer cells survive in the circulation. 4) Extravasation; cancer cells exit the vessel and seed at a distant site after crossing the vessel wall. 5) Secondary tumor development. (B) Biochemical cues; oxygen and nutrient levels are lower, while acidity and carbon dioxide levels are higher within the tumor. (C) Cellular cues, from cells such as fibroblasts, immune cells, and endothelial cells. (D) The extracellular matrix (ECM); the structure and biochemical properties of the ECM fibers (green lines) is heterogeneous in the TME. (E) Mechanical cues, including interstitial fluid pressure and flow, tissue stresses and deformations.

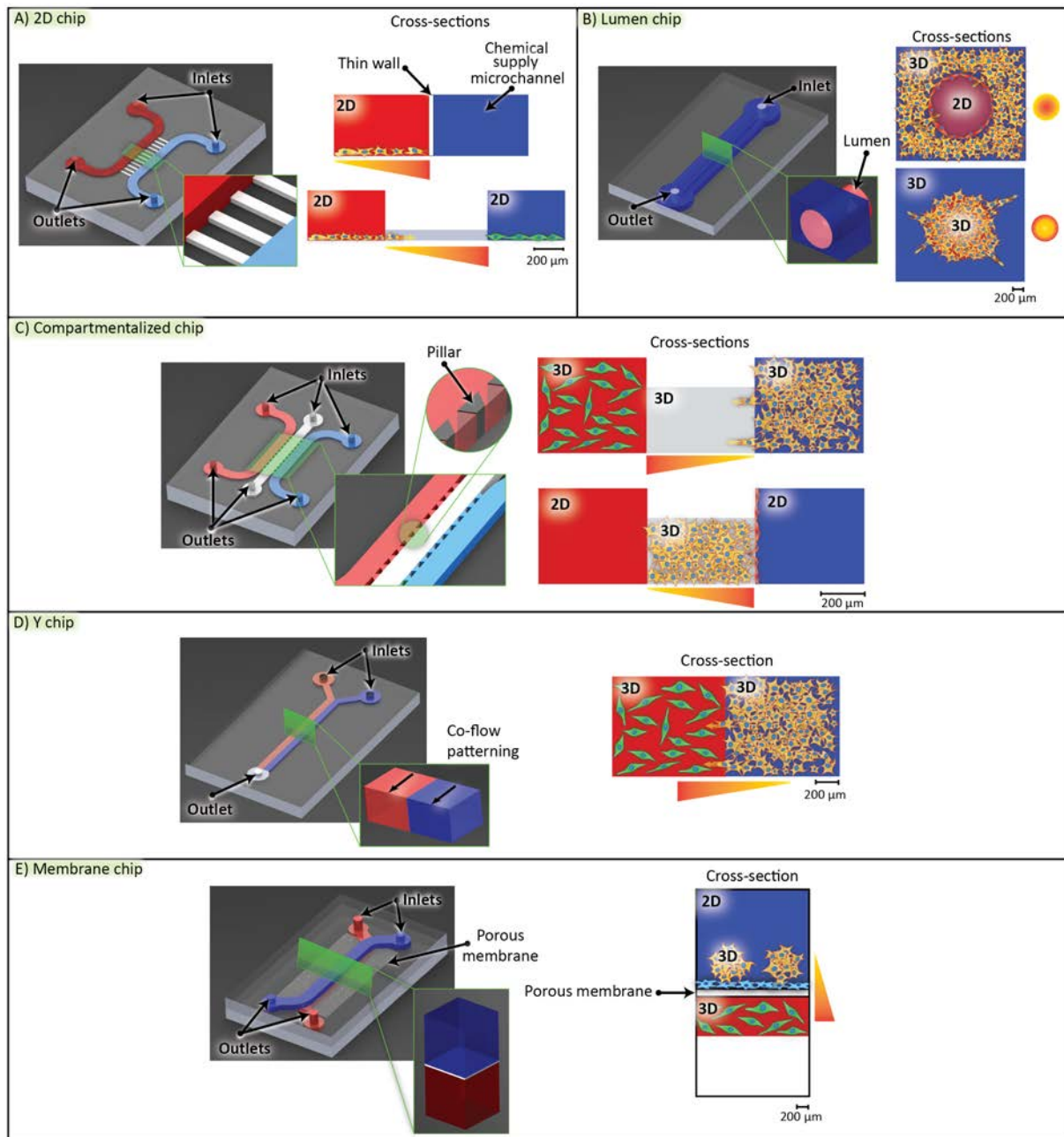


Figure 2: – Cancer-on-a-chip designs with different cell culture options. The complete chips are typically a few cm in size: (A) **2D chip**; Single- or multi-chamber 2D culture devices with a controlled solute gradient. In this type of chip, cancer cells are typically exposed to a gradient of a solute, such as oxygen, while their viability or migration is measured. (B) **Lumen chip**; a patterned 3D matrix is used to form lumens or tumor compartments. This design is typically used to model blood vessels in tumors, or to tightly pack cancer cells in a cylindrical compartment. (C) **Compartmentalized chip**; in this device, pillars are used to separate microchannels in which cell culturing is possible in both 2D and 3D. This type of chip is very versatile, allowing the user to pattern different matrix materials and cells in a controlled manner. (D) **Y chip**; parallel matrix compartments patterned by co-flow. This chip type resembles the compartmentalized chip, as it enables matrix patterning, but is slightly less versatile in its patterning possibilities. (E)

Membrane chip; a co-culture device with stacked microchannels separated by a porous membrane. This multi-layered chip type was originally developed to mimic the endo- and epithelial cell layers found in the lung. In all images, cancer cells are indicated in yellow, additional cell types in red, green, or blue, and solute gradient directions as yellow-red gradients. All scale bars indicate $\pm 200 \mu\text{m}$.

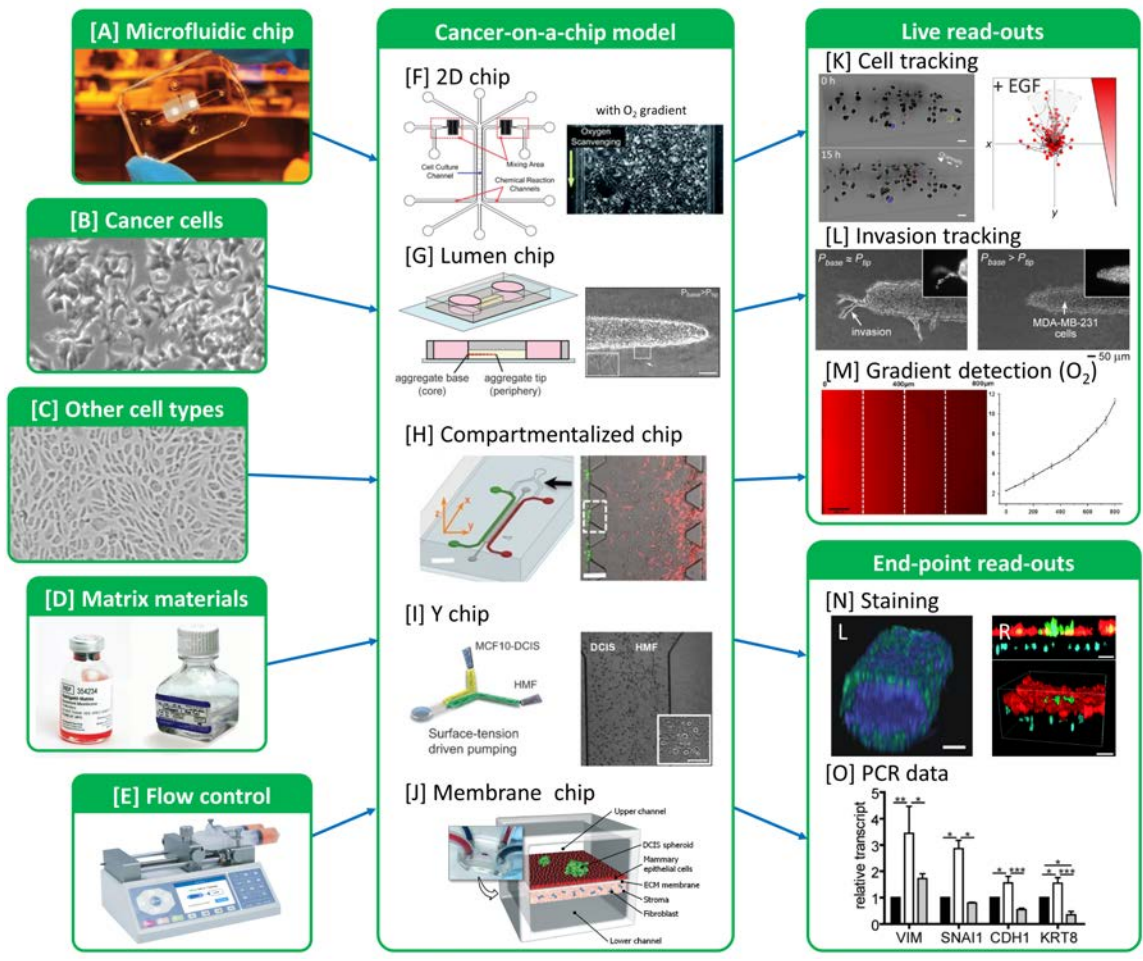


Figure 3 – Cancer-on-a-chip in practice: The key input elements of CoC models are (A) a microfluidic chip, (B) cancer cells, (C) additional cells (optional), (D) matrix materials (optional), and (E) equipment to control fluid flow, such as a syringe pump. Using these elements, the different CoC model types can be built: (F) 2D chips, adapted from (Chen et al., 2011) with permission from The Royal Society of Chemistry, (G) Lumen chips, adapted from (Piotrowski-Daspit et al., 2016) with permission from The Royal Society of Chemistry, (H) Compartmentalized chips (Zervantonakis et al., 2012), (I) Y chips, adapted from (Sung et al., 2011) with permission from The Royal Society of Chemistry, and (J) membrane chips, adapted from (Choi et al., 2015) with permission from The Royal Society of Chemistry. Different experimental read-outs are possible, with some typical examples shown in K-O. The main strength of the CoC approach is that it allows continuous live monitoring of model development: (K) Individual cells (Truong et al., 2016), and (L) invasive lesions can be tracked (Tien et al., 2012). (M) Solute levels can be tracked, adapted from (Wang et al., 2015a) with permission from Springer Nature. These live read-outs can be combined with end-point read-outs, such as tissue staining, shown in (NL) (Bischel et al., 2015) and (NR), adapted from (Choi et al., 2015) with permission from The Royal Society of Chemistry, and (O) gene expression data, adapted from (Piotrowski-Daspit et al., 2016) with permission from The Royal Society of Chemistry.